Journal of Solid Mechanics Vol. 2, No. 2 (2010) pp. 144-155

Inhomogeneity Material Effect on Electromechanical Stresses, Displacement and Electric Potential in FGM Piezoelectric Hollow Rotating Disk

A. Ghorbanpour Arani [1,*], H. Khazaali[1], M. Rahnama[1], M. Dadkhah[2]

[1]*Department of Mechanical Engineering, Faculty of Engineering, University of Kashan, Kashan, Iran*
[2]*Department of Mechanical Engineering, Khomeynishahr Branch, Islamic Azad University, Khomeynishahr, Iran*

Received 17 May 2010; accepted 19 July 2010

ABSTRACT
In this paper, a radially piezoelectric functionally graded rotating disk is investigated by the analytical solution. The variation of material properties is assumed to follow a power law along the radial direction of the disk. Two resulting fully coupled differential equations in terms of the displacement and electric potential are solved directly. Numerical results for different profiles of inhomogeneity are also graphically displayed.

Keywords: Functionally graded material; Piezoelectric; Rotating disk; Analytical solution

1 INTRODUCTION

RECENTLY, applications of advanced materials such as piezoelectrics, functionally graded materials, etc. have become of great importance in high-technology industries. Literature on the subject includes Tiersten [1], Berlincourt [2], Berlincourt et al. [3], Jaffe et al. [4], and Grinchenko et al. [5]. In these media, obtaining material behavior requires either solution of multi-field interactions such as elastic and electric fields in homogeneous piezoelectrics, or consideration of heterogeneity in functionally graded materials (FGMs), or both, as in functionally graded piezoelectric materials (FGPM). Adelman et al. [6] investigated the problem of vibration of a long piezoelectric homogeneous cylinder. The effect of time dependency because of time-harmonic loading is reduced to frequency of the applied load, which was quantified analytically. Khoshgoftar et al. [7] investigated the thermo elastic behavior of a thick walled cylinder with functionally graded materials. The cylinder was loaded under the temperature gradient and inner and outer pressure. Bayat et al. [8] studied elastic solutions for axisymmetric rotating disks made of functionally graded material with variable thickness.

Introducing the displacements function, Chen [9] simplified the governing differential equations in radially polarized piezoelectricmedia and converted them to ordinary Euler differential equations. Ghorbanpour et al. [10] studied the radially polarized spherically anisotropic piezoelectric material under internal and external uniform pressure and a constant potential difference between its inner and outer surfaces of the sphere induce the potential difference. Hou et al. [11] solved the transient problem of a functionally graded magneto-electro-elastic hollow cylinder. The solution was carried out by introducing a new dependent variable and employing the separation of variables technique as well as the superposition method. Babaei et al. [12] considered the analytical solution for radially piezoelectric functionally graded rotating hollow shaft. The variation of material properties assumed to follow a power law along the radial direction of the shaft.

In this study, the influence of inhomogeneity material on a FGPM hollow rotating disk is examined.

* Corresponding author. Tel.: +98 913 162 6594; fax: +98 361 559 930.
E-mail address: aghorban@kashanu.ac.ir; a_ghorbanpour@yahoo.com (A. Ghorbanpour Arani).

2 FUNDAMENTAL EQUATIONS

Here, we consider a functionally graded (FG) piezoelectric disk rotating at a constant angular velocity ω as shown in Fig. 1. The disk has an inner and outer radiuses that are a and b, respectively. The disk is subjected to electric potentials of φ_a and φ_b, respectively, on the inner and outer surfaces. It is assumed that the physical properties of the shaft vary according to a power law along the radial direction as follows

$$X(r) = X_0 \left(\frac{r}{b}\right)^{2N} \tag{1}$$

In which $X(r)$ is the general properties of the disk such as the elastic, piezoelectric, and dielectric coefficients, and X_0 is related with the value of the coefficients at the outer surface. For a piezoelectric medium, the constitutive relations are as follows [6]

$$\begin{aligned} \sigma_{rr} &= C_{33}\bar{\varepsilon}_{rr} + C_{13}\bar{\varepsilon}_{\theta\theta} - e_{33}E_r \\ \sigma_{\theta\theta} &= C_{13}\bar{\varepsilon}_{rr} + C_{11}\bar{\varepsilon}_{\theta\theta} - e_{31}E_r \\ D_r &= e_{33}\bar{\varepsilon}_{rr} + e_{31}\bar{\varepsilon}_{\theta\theta} + \varepsilon_{33}E_r \end{aligned} \tag{2}$$

where σ_{rr}, $\sigma_{\theta\theta}$, D_r, $\bar{\varepsilon}_{rr}$, and $\bar{\varepsilon}_{\theta\theta}$ are the components of the stress, electric displacement, and strain, respectively, C_{ijkl}, e_{kij}, and ε_{ik} are material properties, namely, the elastic, piezoelectric, and dielectric constants. For an axisymmetric problem using linear elasticity we have for strains

$$\bar{\varepsilon}_{rr} = \frac{\partial u}{\partial r}, \qquad \bar{\varepsilon}_{\theta\theta} = \frac{u}{r}, \qquad E_r = -\frac{\partial \phi}{\partial r} \tag{3}$$

In which u and φ are the radial displacements and electric potential, respectively. Also, r and θ are the radial and circumferential coordinates, respectively. For cylindrically orthotropic piezoelectric materials polarized in the radial direction, Eqs. (2) can be written as

$$\begin{aligned} \sigma_{rr} &= C_{33}\frac{\partial u}{\partial r} + C_{13}\frac{u}{r} + e_{33}\frac{\partial \phi}{\partial r} \\ \sigma_{\theta\theta} &= C_{13}\frac{\partial u}{\partial r} + C_{11}\frac{u}{r} + e_{31}\frac{\partial \phi}{\partial r} \\ D_r &= e_{33}\frac{\partial u}{\partial r} + e_{31}\frac{u}{r} - \varepsilon_{33}\frac{\partial \phi}{\partial r} \end{aligned} \tag{4}$$

On the other hand, the equation of motion and the Maxwell equation in the absence of body forces and free charge density read

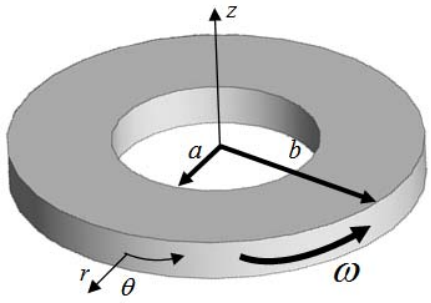

Fig. 1
Geometry and boundary conditions of an FGM piezoelectric disk.

$$\frac{\partial \sigma_{rr}}{\partial r}+\frac{\sigma_{rr}-\sigma_{\theta\theta}}{r}+\rho_d(r)r\omega^2=0$$
$$div(D)=\frac{\partial(rD_r)}{r\partial r}=0\rightarrow\frac{\partial D_r}{\partial r}+\frac{D_r}{r}=0 \tag{5}$$

where ρ_d is the spatially varying mass density of the disk.

3 EXACT SOLUTION

3.1 Governing equations

Using Eqs. (1), (4) and (5), according to D. Alembert's principle, two coupled governing differential equations for the problem are obtained

$$r^2C_{330}u_{,rr}+r(2N+1)\ C_{330}u_{,r}+(2NC_{130}-C_{110})u+r^2e_{330}\phi_{,rr}+r\left[(2N+1)e_{330}-e_{310}\right]\phi_{,r}+\rho_{d0}r^3\omega^2=0$$
$$r^2e_{330}u_{,rr}+r\left[(2N+1)\ e_{330}+e_{310}\right]u_{,r}+2Ne_{310}u-r^2\varepsilon_{330}\phi_{,rr}-r(2N+1)\varepsilon_{330}\phi_{,r}=0 \tag{6}$$

where ω is the angular velocity of the disk, which is taken to be constant. By introducing new dimensionless values as follows

$$\alpha=\frac{C_{110}}{C_{330}},\qquad \beta=\frac{e_{310}}{e_{330}},\qquad \theta=\frac{C_{130}}{C_{330}},\qquad \gamma=\frac{\varepsilon_{330}C_{330}}{e^2{}_{330}} \tag{7}$$

and a new electric potential

$$\Phi=\frac{e_{330}}{C_{330}}\phi \tag{8}$$

Eqs. (6) can be rewritten as

$$r^2u_{,rr}+r(2N+1)u_{,r}+(2N\theta-\alpha)u+r^2\Phi_{,rr}+r\left[(2N+1)-\beta\right]\phi_{,r}+\frac{\rho_{d0}r^3\omega^2}{C_{330}}=0$$
$$r^2u_{,rr}+r\left[(2N+1)+\beta\right]u_{,r}+2N\beta u-r^2\gamma\Phi_{,rr}-r(2N+1)\ \gamma\Phi_{,r}=0 \tag{9}$$

By replacing the radial coordinate with the nondimensionalized radial coordinate $\rho=r/a$ and using the chain rule for differentiation, Eqs. (9) can be rearranged as follows

$$\rho^2u_{,\rho\rho}+\rho(2N+1)u_{,\rho}+(2N\theta-\alpha)u+\rho^2\Phi_{,\rho\rho}+\rho(2N+1-\beta)\phi_{,\rho}+\frac{\rho_{d0}\rho^3\omega^2a^3}{C_{330}}=0$$
$$\rho^2u_{,\rho\rho}+\rho(2N+1+\beta)u_{,\rho}+2N\beta u-\rho^2\gamma\Phi_{,\rho\rho}-\rho(2N+1)\gamma\Phi_{,\rho}=0 \tag{10}$$

The above equations are coupled ordinary differential equations with variable coefficients about u and φ. Here, we use the change of variable $\rho=e^{\eta}$ to convert the equations to new equations with constant coefficients. After some manipulations, we have

$$\ddot{u}+2N\dot{u}+(2N\theta-\alpha)u+\ddot{\Phi}+(2N-\beta)\dot{\Phi}=-\Omega ae^{3\eta}$$
$$\ddot{u}+(2N+\beta)\dot{u}+2N\beta u-\gamma\ddot{\Phi}-2N\gamma\dot{\Phi}=0 \tag{11}$$

in which

$$\Omega = \frac{\rho_{d0}\rho^3\omega^2 a^3}{C_{330}} \tag{12}$$

is the rotational term and an over-dot stands for differentiation with respect to η. After elimination of $\ddot{\Phi}$ between Eqs. (11) and solving for $\dot{\Phi}$, we have

$$\dot{\Phi} = \frac{\gamma+1}{\beta\gamma}\ddot{u} + \frac{2N(1+\gamma)+\beta}{\beta\gamma}\dot{u} + \frac{2N(\beta+\theta\gamma)-a\gamma}{\beta\gamma}u + \frac{\Omega a}{\beta}e^{3\eta} \tag{13}$$

Substituting the above relation and its derivative into the first equation of Eqs. (11), the decoupled equation about u is obtained as follows

$$a_3\dddot{u} + a_2\ddot{u} + a_1\dot{u} + a_0 u = de^{3\eta} \tag{14}$$

where

$$\begin{aligned} a_3 &= -\frac{\gamma+1}{\beta}, \qquad a_2 = -\frac{4N(\gamma+1)}{\beta}, \qquad a_1 = 2N+\beta-\frac{2N(\beta+\theta\gamma)-a\gamma}{\beta}-\frac{4N^2(1+\gamma)+2\beta N}{\beta} \\ a_0 &= -2N\beta-\frac{4N^2(\beta+\theta\gamma)-2a\gamma N}{\beta}, \qquad d = \frac{\Omega\gamma a(3+2N)}{\beta} \end{aligned} \tag{15}$$

The general solution of Eq. (14) is

$$u_g = Ae^{m_1\eta} + Be^{m_2\eta} + Ce^{m_3\eta} \tag{16}$$

in which m_i (i = 1, 2, 3) are the roots of the corresponding characteristic equation of Eq. (14). A, B, and C are integration constants to be determined by boundary conditions. The particular solution of Eq. (14) is assumed to have the form $u_p = Ke^{3\eta}$. After substitution of the assumed particular solution and its derivatives into Eq. (14), K is found

$$K = \frac{d}{27a_3+9a_2+3a_1+a_0} \tag{17}$$

So, the final solution for u in terms of the nondimensionalized radial coordinate is

$$u = u_g + u_p = A\rho^{m_1} + B\rho^{m_2} + C\rho^{m_3} + K\rho^3 \tag{18}$$

Substituting for u from the above equation into Eq. (13) and integrating, Φ is also obtained

$$\Phi = b_1 A\rho^{m_1} + b_2 B\rho^{m_2} + b_3 C\rho^{m_3} + D + f\rho^3 \tag{19}$$

where D is a new integration constant and

$$b_i = \frac{1}{\beta\gamma}\left((1+\gamma)m_i + 2N(1+\gamma) + \beta + \frac{2N(\beta+\theta\gamma)-a\gamma}{m_i}\right), \qquad i = 1,2,3 \tag{20a}$$

$$f=\frac{1}{\beta\gamma}\left(K((\gamma+1)(3+2N)+\beta+2N(\beta+\theta\gamma)-a\gamma)+\frac{\Omega a\gamma}{3}\right) \tag{20b}$$

It is more convenient to nondimensionalize stresses and electric potential as follows

$$\sum\nolimits_{rr}=\frac{\sigma_{rr}}{C_{330}},\qquad \sum\nolimits_{\theta\theta}=\frac{\sigma_{\theta\theta}}{C_{330}},\qquad \Phi_1=\frac{\Phi}{a} \tag{21}$$

Then, using Eqs. (4), (18), and (19) we have

$$\begin{aligned}
\sum\nolimits_{rr}&=\mu^{2N}\frac{\rho^{2N-1}}{a}(A\rho^{m_1}(m_1+\theta+b_1m_1)+B\rho^{m_2}(m_2+\theta+b_2m_2)\\
&\quad+C\rho^{m_2}(m_3+\theta+b_3m_3)+\rho^3(K(3+\theta)+3f))\\
\sum\nolimits_{\theta\theta}&=\mu^{2N}\frac{\rho^{2N-1}}{a}(A\rho^{m_1}(\theta m_1+\alpha+\beta b_1m_1)+B\rho^{m_2}(\theta m_2+\alpha+\beta b_2m_2)\\
&\quad+C\rho^{m_2}(\theta m_3+\alpha+\beta b_3m_3)+\rho^3(K(3\theta+\alpha)+3\beta f))\\
\Phi_1&=\frac{b_1}{a}A\rho^{m_1}+\frac{b_2}{a}B\rho^{m_2}+\frac{b_3}{a}C\rho^{m_3}+\frac{D}{a}+\frac{f}{a}\rho^3\\
u_1&=\frac{A}{a}\rho^{m_1}+\frac{B}{a}\rho^{m_2}+\frac{C}{a}\rho^{m_3}+\frac{K}{a}\rho^3
\end{aligned} \tag{22}$$

in which $\mu=a/b$ is the aspect ratio.

3.2 Boundary conditions and solution

According to Fig. 1, the boundary conditions can be defined in the following form

$$\begin{aligned}
&\sum\nolimits_{rr}(1)=\sum\nolimits_{rri} \qquad \Phi_1(1)=\Phi_{1i} \qquad u_1(1)=u_{1i}\\
&\sum\nolimits_{rr}(\mu)=\sum\nolimits_{rro} \qquad \Phi_1(\mu)=\Phi_{1o}
\end{aligned} \tag{23}$$

Using Eqs. (22) and (23) we have a set of four linear algebraic equations for the four unknowns, *A*, *B*, *C*, and *D*, as follows

$$P\begin{Bmatrix}A\\B\\C\end{Bmatrix}=Q \tag{24}$$

where, *P* is a 4 × 4 nontrivial matrix.

4 NUMERICAL SOLUTION

In this section, numerical results are presented graphically for radial and circumferential stresses, electric potential and displacement. The outer surface of the disk is assumed to be PZT-4 whose properties are listed in the Table 1. Figures depicted the effect of inhomogeneity on the results for aspect ratios μ=1.3. The rotational term Ω is also taken to be unity.

Table 1
Properties of PZT-4

Coefficient	PZT-4
C_{330}	115×10^9 Pa
C_{110}	139×10^9 Pa
C_{130}	74.3×10^9 Pa
e_{310}	- 5.20 C/m^2
e_{330}	15.1 C/m^2
ε_{330}	5.62×10^{-9} F/m
ρ_{d0}	7.5×10^3 kg/m^3

5 RESULTS AND DISCUSSIONS

According to the figures, following results are achieved. Fig. 1 displays the radial stresses in free-free state with no electric potential related with dimensionless radius. Corresponding with the boundary conditions, stresses on the inner and outer radiuses are zero and those have a maximum between inner and outer radius. The more the nonhomogenous parameter *N* increases the more the stresses will be.

Fig. 2 displays the circumferential stresses in free-free state with no electric potential related with dimensionless radius. The stresses increase as the nonhomogenous parameter *N* increases. It is possible that a fracture occurs in high amount of *N*. Fig. 3 displays the electric potentials related with dimensionless radius. As the nonhomogenous parameter is negative, electric potential has a minimum; on the contrary, it has a maximum when nonhemogenous parameter is positive. Fig. 4 displays the radial displacements related with dimensionless radius. These displacements are maximum in inner radius and minimum in outer radius and increase as the nonhomogenous parameter increases. Figs. 5-8 are radial stresses, circumferential stresses, electric potentials and radial displacements in free-free state respectively. Here, we have unit electric potential on inner radius and zero electric potential on outer radius. The results are the same as above. Figs. 9-12 are radial stresses, circumferential stresses, electric potentials and radial displacements in free-free state respectively. Here, we have unit electric potential on outer radius and zero electric potential on inner radius. Fig. 9 displays the radial stresses that decrease as the nonhomogenous parameter increases. Fig. 10 shows the circumferential stresses that increase as the nonhomogenous parameter increases. Fig. 11 exhibits the electric potential that increase as the nonhomogenous parameter increases. Fig. 12 presents the radial displacements that are the same as above and increase as the nonhomogenous parameter increases.

Figs. 13-16 are radial stresses, circumferential stresses, electric potentials and radial displacements in fixed-free state respectively. Here, we have zero electric potential on outer and inner radiuses. Fig. 13 displays the radial stresses that are descendant and increase as the nonhomogenous parameter increases. Fig. 14 depicts the circumferential stresses that are ascendant and increase as the nonhomogenous parameter increases. Fig. 15 shows the electric potentials that increase as the nonhomogenous parameter increases. Fig. 16 manifests the ascendant radial displacements. According to the boundary condition, radial displacement is zero on inner radius. As the nonhomogenous parameter increases the radial displacements increase. Figs. 17-20 are radial stresses, circumferential stresses, electric potentials and radial displacements in fixed-free state respectively. Here, we have unit electric potential on inner radius and zero electric potential on outer radius. Fig. 17 displays the radial stresses that are descendant and increase as the nonhomogenous parameter increases. Fig. 18 shows the circumferential stresses. Slope of the diagrams increase as the nonhomogenous parameter increases. Fig. 19 depicts the electric potentials that increase as the nonhomogenous parameter increases. Fig. 20 shows the ascendant radial displacements. According to the boundary condition, radial displacement is zero on inner radius. As the nonhomogenous parameter increases the radial displacements increase.

Figs. 21-24 are radial stresses, circumferential stresses, electric potentials and radial displacements in fixed-free state respectively. Here, we have unit electric potential on outer radius and zero electric potential on inner radius. Fig. 21 displays the radial stresses that are descendant and increase as the nonhomogenous parameter increases. Fig. 22 shows the circumferential stresses that are ascendant and increase as the nonhomogenous parameter increases. Fig. 23 depicts the electric potentials that increase as the nonhomogenous parameter increases. Fig. 24 presents the radial displacements. According to the boundary condition, radial displacement is zero on inner radius. As the nonhomogenous parameter increases the radial displacements increase. The assumed mechanical and electrical boundary conditions of the disk are:

For free-free state

Case 1: $\sum_{rr}(1)=0, \quad \sum_{rr}(\mu)=0, \quad \Phi_1(1)=0, \quad \Phi_1(\mu)=0$

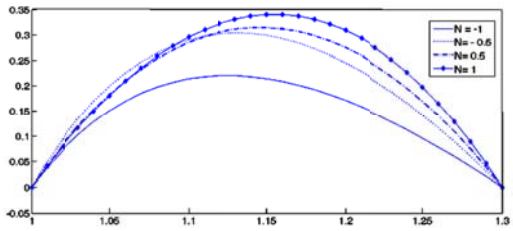

Fig. 1
Radial stress for different N, Ω=1, μ=1.3.

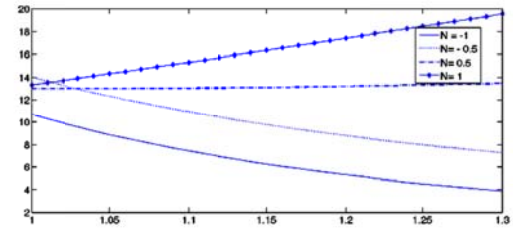

Fig. 2
Circumferential stresses for different N, Ω=1, μ=1.3.

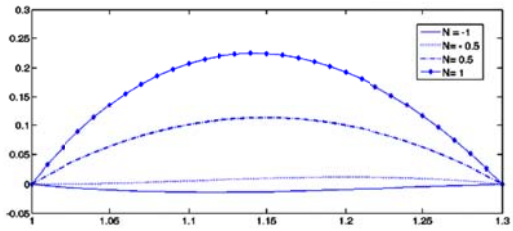

Fig. 3
Electric potential for different N, Ω=1, μ=1.3.

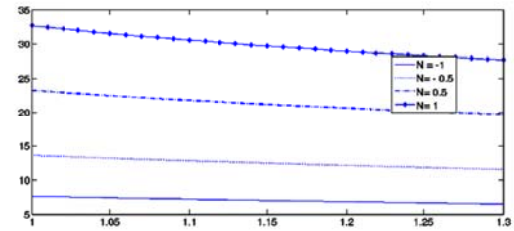

Fig. 4
Radial displacement for different N, Ω=1, μ=1.3.

Case 2: $\sum_{rr}(1)=0, \quad \sum_{rr}(\mu)=0, \quad \Phi_1(1)=1, \quad \Phi_1(\mu)=0$

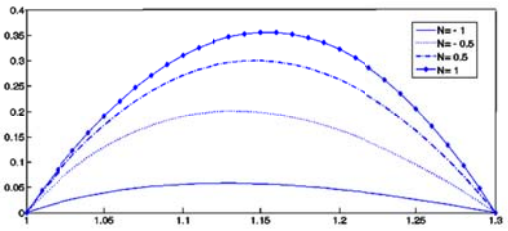

Fig. 5
Radial stress for different N, Ω=1, μ=1.3.

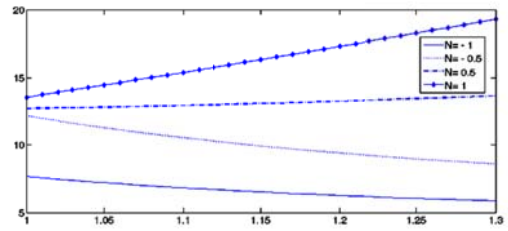

Fig. 6
Circumferential stresses for different N, Ω=1, μ=1.3.

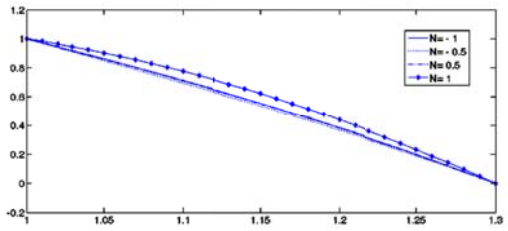

Fig. 7
Electric potential for different N, Ω=1, μ=1.3.

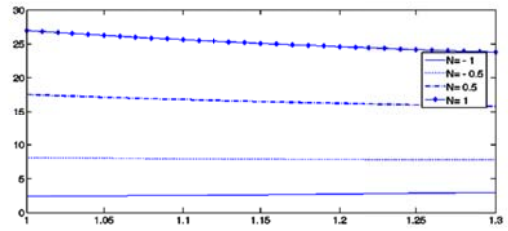

Fig. 8
Radial displacement for different N, Ω=1, μ=1.3.

Case 3: $\sum_{rr}(1)=0, \quad \sum_{rr}(\mu)=0, \quad \Phi_1(1)=0, \quad \Phi_1(\mu)=1$

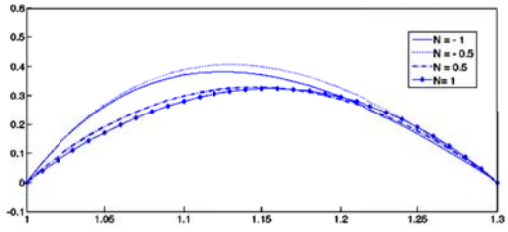

Fig. 9
Radial stress for different N, Ω=1, μ=1.3.

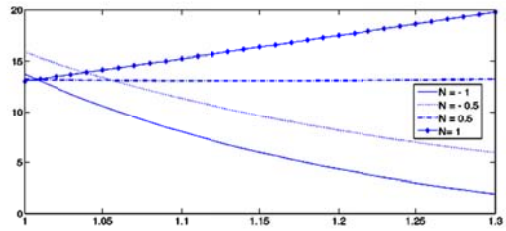

Fig. 10
Circumferential stresses for different N, Ω=1, μ=1.3.

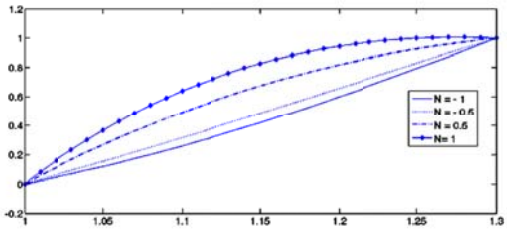

Fig. 11
Electric potential for different N, Ω=1, μ=1.3.

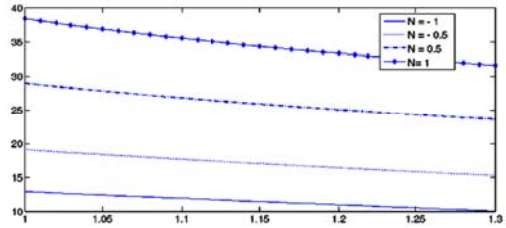

Fig. 12
Radial displacement for different N, Ω=1, μ=1.3.

For fixed-free state

Case 1: $u_1(1) = 0 \qquad \sum_{rr}(\mu) = 0, \qquad \Phi_1(1) = 0, \qquad \Phi_1(\mu) = 0$

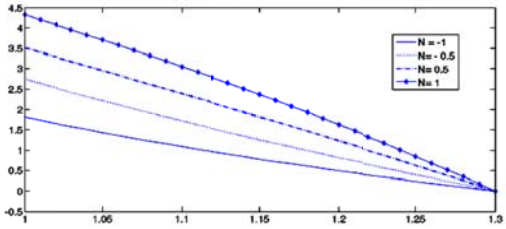

Fig. 13
Radial stress for different N, Ω=1, μ=1.3.

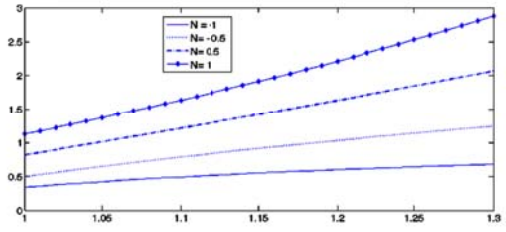

Fig. 14
Circumferential stresses for different N, Ω=1, μ=1.3.

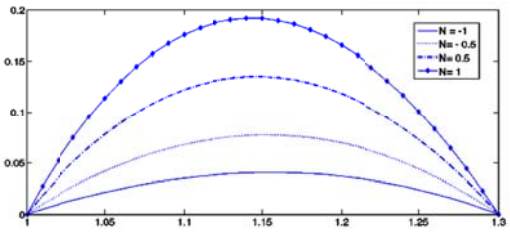

Fig. 15
Electric potential for different N, Ω=1, μ=1.3.

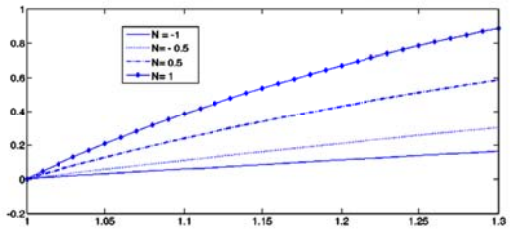

Fig. 16
Radial displacement for different N, Ω=1, μ=1.3.

Case 2: $u_1(1) = 0 \qquad \sum_{rr}(\mu) = 0, \qquad \Phi_1(1) = 1, \qquad \Phi_1(\mu) = 0$

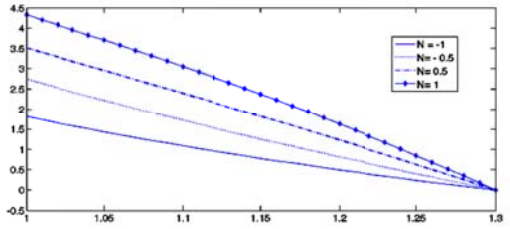

Fig. 17
Radial stress for different N, Ω=1, μ=1.3.

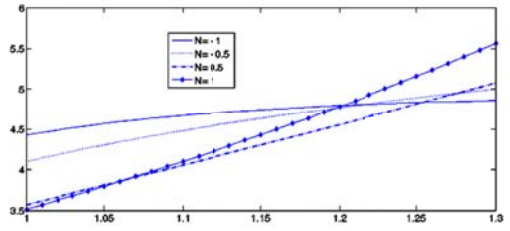

Fig. 18
Circumferential stresses for different N, Ω=1, μ=1.3.

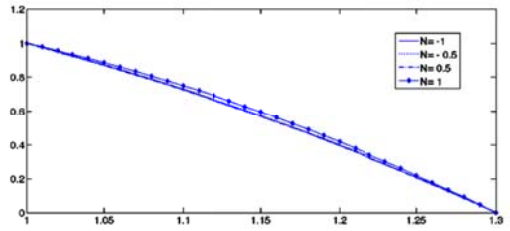

Fig. 19
Electric potential for different N, Ω=1, μ=1.3.

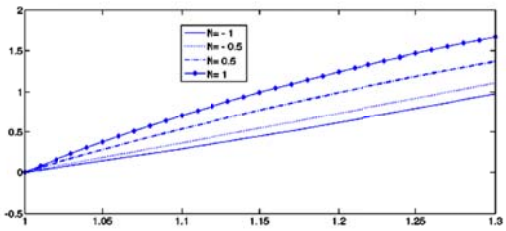

Fig. 20
Radial displacement for different N, Ω=1, μ=1.3.

Case 3: $u_1(1)=0 \qquad \sum_{rr}(\mu)=0, \qquad \Phi_1(1)=0, \qquad \Phi_1(\mu)=1$

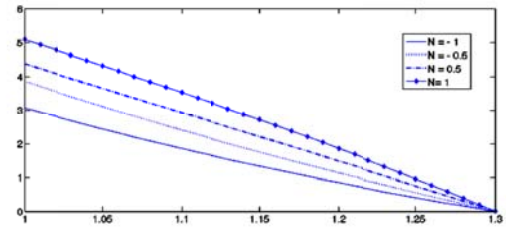

Fig. 21
Radial stress for different N, Ω=1, μ=1.3.

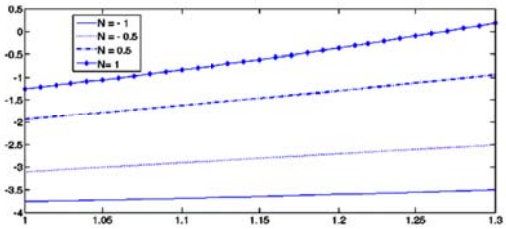

Fig. 22
Circumferential stresses for different N, Ω=1, μ=1.3.

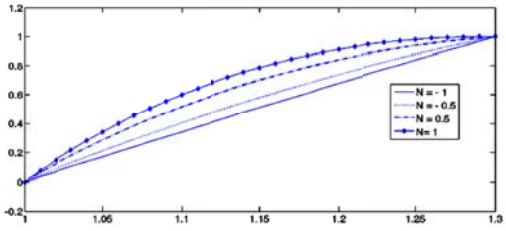

Fig. 23
Electric potential for different N, Ω=1, μ=1.3.

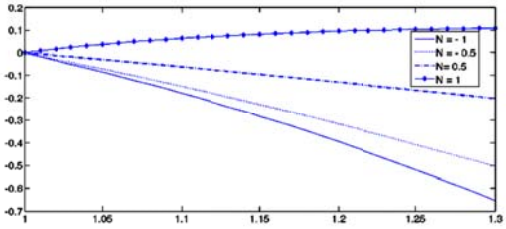

Fig. 24
Radial displacement for different N, Ω=1, μ=1.3.

6 CONCLUSIONS

In the present paper, an exact solution for a rotating disk made of FGPM under mechanical loads was derived using the elasticity theory by assuming power functions for all properties. The appropriate mechanical and electrical equations were derived for solving the piezoelectric problem. On finding the numerical value of the solution to the problem, the following conclusions are obtained:

1. Radial stress, circumferential stress, electric potential and radial displacement increase on increasing nonhomogeneous parameter.
2. In free-free state with no electric potential, internal electric potential and external electric potential, circumferential stress is positive and it causes fatigue fracture.
3. In fixed-free state with no electric potential and internal electric potential, circumferential stress is positive and it causes fatigue fracture, while circumferential stress is negative and it prevents fatigue fracture, with external electric potential; therefore, it is the best boundary conditions and loading.
4. In free-free state with internal electric potential, circumferential stress and radial displacement decrease.
5. In fixed-free state circumferential stress, radial stress and radial displacement are less than free-free state.

REFERENCES

[1] Tiersten H.F., 1969, *Linear Piezoelectric Plate Vibrations*, Plenum, New York.

[2] Berlincourt D.A., 1971, Piezoelectric crystals and ceramics, in: *Ultrasonic Transducer Materials*, edited by *O.E. Mattiat,* Plenum, New York, 63-124.

[3] Berlincourt D.A., Curran D.R., Jaffe H., 1964, Piezoelectric and piezomagnetic materials and their function in transducers, in: *Physical Acoustics: Principles and Methods*, edited by W.P. Mason, Academic, New York, 169-270.

[4] Jaffe B., Cook W.R. Jr, Jaffe H., 1971, *Piezoelectric Ceramics*, Academic, London.

[5] Grinchenko V.T., Ulitko A.F., Shul'ga N.A., 1989, Electroelasticity, In: *Mechanics of Coupled Fields in Structural Members (in Russian)*, edited by A.N. Guz, (ed.), Volume 5 of the five-volume series, Naukova Dumka, Kiev.

[6] Adelman N.T., Stavsky Y., Segal E., 1975, Axisymmetric vibrations of radially polarized piezoelectric ceramic cylinders, *Journal of Sound and Vibration* **38**: 245-254.

[7] Khoshgoftar M.J., Ghorbanpour, A., Arefi, M., 2009, Thermoelastic analysis of thick walled cylinder made of functionally graded piezoelectric material, *Smart Materials and Structures* **18**: 115007.

[8] Bayat M., Saleem M., Sahari B.B., Hamouda A.M.S., Mahdi E., 2007, Analysis of functionally graded rotating disks with variable thickness, *Thin-Walled Structures* **45**(7-8): 677-691

[9] Chen, W.Q., 1999, Problems of radially polarized piezoelastic bodies, *International Journal of Solids and Structures* **36**: 4317-4332.

[10] Ghorbanpour A., Golabi S., Saadatfar M., 2006, Stress and Electric Potential Fields in piezoelectric Smart Spheres, *Journal of Mechanical Science and Technology* **20**: 1920-1933.

[11] Hou P.F., Ding H.J., Leung A.Y.T., 2006, The transient responses of a special inhomogeneous magneto-electro-elastic hollow cylinder for axisymmetric plane strain problem, *Journal of Sound and Vibration* **291**: 19-47.

[12] Babaei M.H., Chen Z.T., 2008, Analytical solution for the electromechanical behavior of a rotating functionally graded piezoelectric hollow shaft, *Archive of Applied Mechanics* **78**: 489-500.